THE ASTROPHYSICAL JOURNAL, 471:L23–L26, 1996 November 1

THE FIRST SPECTROSCOPIC OBSERVATIONS OF CAUSTIC CROSSING IN A BINARY MICROLENSING EVENT[1]

DANIEL J. LENNON[2] AND SHUDE MAO
Max-Planck-Institut für Astrophysik, Karl-Schwarzschild-Strasse 1, D-85740 Garching, Germany

AND

K. FUHRMANN AND T. GEHREN
Universitäts-Sternwarte, Scheinerstrasse 1, D-81679 Munich, Germany
Received 1996 June 18; accepted August 9

ABSTRACT

We present the first spectroscopic observations of a binary microlensing event when it was undergoing a caustic crossing with a high magnification of $A \approx 25$. The event 96-BLG-3 was identified in real time by the MACHO collaboration, in the Baade's window field toward the Galactic bulge. Three spectra were taken consecutively, spanning the light-curve peak of the caustic crossing, each integration lasting 30 minutes. The spectrograms covered the wavelength range 3985–6665 Å and are almost identical, the third one differing only in having an amplitude ≈6% lower than the others. By comparison with reference star spectra and by using spectrum synthesis techniques, we infer that the source star is a G0 IV–V star, with an effective temperature of $T_{\rm eff} = 6100 \pm 150$ K, a metallicity in the range [M/H] = +0.3 to +0.6, and a logarithmic surface gravity of $\log g = 4.25 \pm 0.25$. Using theoretical evolutionary tracks, we derive a radius of $\approx 1.4^{-0.4}_{+0.6}\ R_\odot$ and hence a distance of $6.9^{-1.7}_{+3.1}$ kpc, consistent with the source residing in the Galactic bulge. We also determine its heliocentric radial velocity to be $v_r = 122 \pm 3$ km s^{-1}. Caustic-crossing microlensing events such as 96-BLG-3, if they are observed with 8–10 m class telescopes, can resolve the stellar surface of distant sources with a resolution of 10^{10} cm or better. This permits a detailed study of the center-to-limb variation of the stellar surface and the intrinsic properties of the lensed source.

Subject headings: dark matter — Galaxy: center — gravitational lensing — stars: abundances — stars: late-type

1. INTRODUCTION

With the aim of searching for dark matter in the Galactic halo (Paczyński 1986), four gravitational microlensing surveys (Alcock et al. 1993, 1996a, 1996b, 1996d [MACHO collaboration]; Udalski et al. 1993, 1994a [OGLE collaboration]; Aubourg et al. 1993 [EROS collaboration]; Alard et al. 1995 [DUO collaboration]) have discovered more than 100 microlensing events toward the Galactic bulge and about 10 events toward the LMC (see Paczyński 1996 for a review). With the implementation of the early warning system (Udalski et al. 1994b) and the alert system (Alcock et al. 1996c), real-time identification of microlensing events has become routine. This allows detailed photometric and spectroscopic observations of ongoing lensing events. The most striking deviations from the standard achromatic, symmetric light curve (Paczyński 1986) are the sharp rises and falls when a source crosses the caustics formed by a binary system (e.g., Mao & Paczyński 1991). So far, four definite binary lensing events have been reported (OGLE 7 [Udalski et al. 1994c; Bennett et al. 1995]; DUO 2 [Alard, Mao, & Guibert 1995]; LMC 9, BLG-95-12 [Pratt 1996; LMC 9 [Bennett et al. 1996]). The first event toward the LMC (Dominik & Hirshfeld 1994) and OGLE 6 (Mao & Di Stefano 1995) may be binaries as well. In this Letter, we present the first real-time spectroscopic observations of a new binary event, BLG-96-3, identified by the alert system of the MACHO collaboration (Alcock et al. 1996e) Previous published spectroscopic observations of microlensing events have been surprisingly rare and are restricted to cases in which the lens is a single object; for instance, Benetti, Pasquini, & West (1995) observed a late G/early K subgiant that underwent a maximum magnification by $A \approx 10.5$. By comparison, the peak magnification factor in the binary lens case discussed here is ≈25 since the source was moving across a caustic at the time of observation.

2. OBSERVATIONS

The binary microlensing candidate, 96-BLG-3, was the third alert event identified in the 1996 season toward the Galactic bulge by the MACHO collaboration.[3] The typical duration for a source to cross a caustic formed by a binary lens is only a few hours, so the crossing is easily missed. Fortunately, caustic crossings always come in pairs; therefore, with the early warning/alert systems, the time of later caustic crossing(s) could in principle be predicted on basis of the light curve before it. In practice, this involves considerable work since the fitting of the light curve could be degenerate, especially for an undersampled light curve (Mao & Di Stefano 1995). Remarkably, this was accomplished for 96-BLG-3 (Alcock et al. 1996e). By coincidence, one of us (D. J. L.) was observing on the night that the fourth caustic crossing in the light curve was predicted to occur. Some time was therefore diverted from the main program so that a spectrum of the source might be obtained.

96-BLG-3 was observed on the night of March 28/29 using

[1] Based on observations taken at the European Southern Observatory, La Silla, Chile.

[2] Current address: Universitäts-Sternwarte, Scheinerstrasse 1, 81679 Munich, Germany.

[3] Information on the MACHO collaboration's alert events can be found at http://darkstar.astro.washington.edu/, including the light curve for 96-BLG-3.

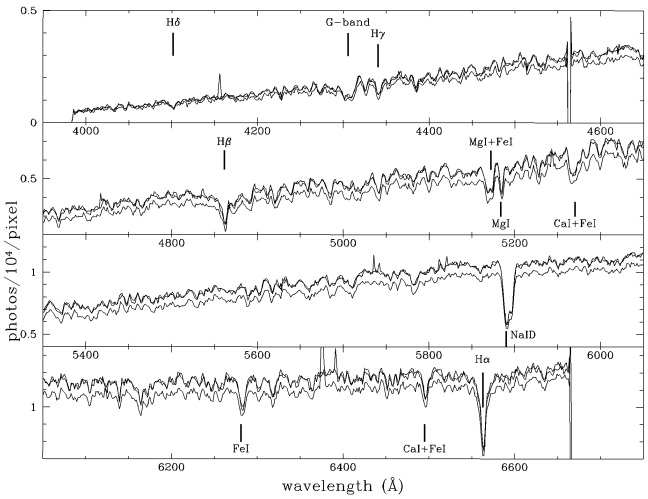

FIG. 1.—The three spectra of the microlensing candidate 96-BLG-3 plotted in four panels. This binary microlensing event was discovered by the MACHO collaboration and was undergoing a caustic crossing with a high magnification of $A \approx 25$. The first and second spectra (*top two curves*) are almost the same, and we did not distinguish them; the third spectrum is the lower curve. Also indicated are some line features. The exposure time for each spectrum was 30 minutes, and the starting time of the observations were JD −2,448,623.5 = 1548.3587, 1548.3825, and 1548.4031. The vertical scale is in units of 10,000 photons pixel^{-1}, with a pixel size of 1.31 Å. All the obvious profile discrepancies are due to either cosmic rays (e.g., at 4160 Å, 6375 Å) or bad columns (e.g., at 4570 Å). Note the tick sizes are the same in all the panels, but the zero points change in both axes.

the ESO New Technology Telescope and the EMMI spectrograph (Melnick, Dekker, & D'Odorico 1994). Three spectrograms were obtained at a nominal resolving power of 1100 (for the 1″ slit employed here). A Tektronix 2048 × 2048 CCD (ESO 34) was used as the detector giving a wavelength coverage of approximately 3985–6665 Å, each 24 μm pixel corresponding to 0.″27 in the spatial direction or about 1.31 Å in the dispersion direction. A slit length of 300 pixels was adopted. The seeing as measured in the spatial direction ranged from 0.″97 in the red to 1.″13 in the blue. Wavelength calibration was carried out using He-Ar arc spectra, the mean value of the residuals (25 lines) was typically 0.1 Å, and the FWHM of the He-Ar emission lines was 4.8 Å. However, since the seeing FWHM was similar to the slit width, the spectral resolution of the stellar spectrum was somewhat higher as a result of the nonuniform illumination of the slit, which corresponds to approximately 3.3 Å FWHM. The integration time for each exposure was 30 minutes, and they were obtained consecutively, interspersed only by CCD readout. The start times of each of the three observations as expressed in the Julian system (JD −2,448,623.5) are 1548.3587, 1548.3825, and 1548.4031 and cover the light-curve peak corresponding to a caustic crossing. The unperturbed visual magnitude of the source star is $V = 19.1 \pm 0.1$; however, during the observations the star had brightened to $V \approx 15.5$. Data reduction was performed within the MIDAS environment using the long-slit reduction package. Note that the third and final spectrogram was taken quite close to morning twilight when there was a noticeable increase in the sky background that was due to scattered sunlight which had to be subtracted from the object. The signal-to-noise ratio (S/N) for each observation depends strongly on wavelength, ranging from 25 in the blue to 100 in the red. The three spectrograms are shown in Figure 1.

3. ANALYSIS

Apart from a small number of features attributable to remnants of cosmic rays, no convincing cases of profile variability were found. The case of continuum variability was not so straightforward since the observations were not spectrophotometric. Nevertheless, we attempted to compensate for this using the brightest of a number of other stars, which were included in the long slit, as a reference frame. Note that these other objects are both fainter than 96-BLG-3 and much redder, making the calibration rather uncertain at the shorter wavelengths (<4500 Å). We found that the first and second spectra have roughly the same amplitude, while the amplitude of the third spectrum is lower by 6%. These scale factors are consistent with the broadband magnification changes during the observations, while the continuum slope changes must be less than 2% in the wavelength range 4500–6600 Å in the three spectra.

In order to constrain the stellar properties more exactly we make use of two additional data sets: (1) a library of high resolution and high S/N spectra of field F- and G-type stars and (2) a grid of synthetic spectra computed with an LTE ODF-blanketed model atmosphere program (see Fuhrmann et al. 1996 for details of the models and stellar parameters). The spectral library data were obtained at Calar Alto using the recently installed FOCES spectrograph at a resolution of 30,000. The synthetic spectra were computed on a fine-wavelength grid ($\Delta\lambda = 0.01$ Å) covering two spectral ranges of 4780–5300 Å and 6460–6660 Å and for the stellar parameters $T_{\rm eff} = 5800$, 6000, 6200, and 6400 K; $\log g = 3.0$, 3.5, 4.0, and 4.5; [M/H] = −0.3, 0.0, +0.3, and +0.6; and a microturbulence of 1 km s^{-1}. Here $T_{\rm eff}$ is the effective temperature, $\log g$ is the logarithm of the surface gravity, and [M/H] refers to the metallicity relative to solar on a logarithmic scale. The first region contains the temperature sensitive Hβ line as well as the luminosity sensitive Mg I triplet at 5167.3, 5172.7, and 5183.6 Å (see Cayrel et al. 1991 for a more detailed discussion of this region). The second wavelength region contains the temperature-sensitive Hα line, which has an advantage over the Hβ line in that it is less affected by blending with metal lines and hence leads to a more metallicity insensitive value for the effective temperature. This line is also intrinsically less sensitive to metallicity and surface gravity (Fuhrmann, Axer, & Gehren 1993).

Before comparing the reference spectra with the 96-BLG-3 data, we convolved them first with an appropriate instrumental broadening function and corrected for radial velocity differences. The radial velocity of 96-BLG-3 was determined by cross-correlating the stellar and sky spectra of the final observation, in the region where the sky is dominated by the solar spectrum (4000–4500 Å). This resulted in a value of 99 ± 3 km s^{-1}, implying radial velocities in the heliocentric and Galactic reference frames of +122 km s^{-1} and +135 km s^{-1}, respectively. Finally, care had to be taken to ensure that various spectra were normalized consistently. This is an important point since, at the resolution of the EMMI data, there is no true continuum and the perceived pseudocontinuum in a given window depends upon the strength and number of the metal lines. Thus, for example, when the normalized high-resolution solar spectrum is convolved to the resolution of 96-BLG-3, the perceived continuum is lowered by between 2% near Hα to 10% at Hγ. The procedure we adopt is to define identical continuum windows for both

reference star and 96-BLG-3 and normalize both spectra using a low-order polynomial (typically a first- or second-order function is adequate).

When we compare the 96-BLG-3 spectrum to that of the field stars, it is clear that its effective temperature and surface gravity must be intermediate between those of the Sun ($T_{\rm eff}$ = 5780 K, log g = 4.44, [M/H] = 0.0) and Procyon ($T_{\rm eff}$ = 6500 K, log g = 4.05, [M/H] = 0.0). These parameters were refined using the grid of synthetic spectra described above but taking into account inaccuracies in the oscillator strengths by comparing a synthetic spectrum with the observed solar spectrum. In deriving the effective temperature we have concentrated on the fit to the Hα line since it is intrinsically insensitive to metallicity and gravity. In addition, the adopted metallicity can influence the position of the pseudocontinuum, an effect which is most severe for the higher Balmer series members where line crowding is greater. In Figure 2 (*top*) we show that the observed Hα line is consistent with an effective temperature of around 6100 K. This is a compromise between the blue wing, which implies 6200 K, and the red wing, which is better fitted with 6000 K. Lower and higher temperatures are clearly ruled out by this comparison. To determine the surface gravity we have relied upon fitting the spectral region around 5100–5300 Å that contains the Mg I triplet. As a result of the many strong metal lines that are also in this region, the derived gravity is somewhat sensitive to the adopted metallicity. However, it was clear that using the [M/H] = −0.3 spectra, we would be forced to adopt a surface gravity well in excess of log g = 4.5. Such a star would lie below the zero-age main sequence in the color-magnitude diagram; in addition, the metal lines were much too weak. The solar metallicity models also implied an uncomfortably large surface gravity, while the metal lines still appear somewhat too weak. The best fits were obtained for [M/H] = +0.3, log g = 4.5 and [M/H] = +0.6, log g = 4.0. To obtain an additional check on the metallicity we selected a blend of primarily Fe I lines (strongest components at 6495, 6496 Å) and Ca I lines (6494, 6500 Å) in a relatively clean part of the spectrum. This blend was well fitted in the solar spectrum, leading us to expect that the implied metallicity should be reliable. At this point we made a further refinement of the synthetic spectra by computing a new set of models with the atomic data adjusted to fit the solar spectrum. This new grid was computed only for the parameter space of immediate interest and for the restricted wavelength ranges 5050–5290 Å and 6480–6520 Å. These improvements were crucial not only in order to derive the metallicity but also to reproduce to the correct behavior of the gravity-sensitive wings of the Mg I triplet. In Figure 2 (*middle*) we show the Ca I/Fe I blend just referred to. This leads us to deduce a metallicity in the range [M/H] = +0.3 to +0.6. Returning to the determination of the surface gravity, the Mg I triplet region then implies a logarithmic surface gravity between 4.0 and 4.5 (Fig. 2, *bottom*). More precisely, [M/H] = +0.3 leads to log g = 4.5, while [M/H] = +0.6 implies log g = 4.0. The many metal lines in this region are also consistent with a metallicity in this range.

Adopting $T_{\rm eff}$ = 6100 K and log g = 4.25 , we can derive a mass and radius for 96-BLG-3 using the evolutionary tracks of Schaerer et al. (1993) transformed to the log g–log $T_{\rm eff}$ plane (these evolutionary tracks were computed using a twice solar metallicity; however, the solar metallicity tracks of Schaller et al. 1992 do not appreciably alter the results). This leads immediately to the mass, the surface gravity then allowing us

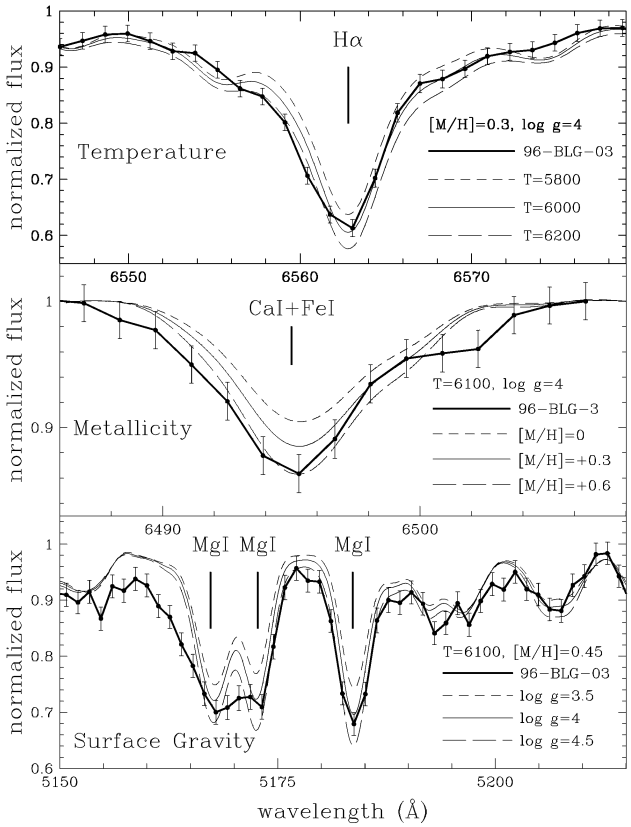

FIG. 2.—Subsections of the spectral regions used to infer the temperature, metallicity, and surface gravity are shown in the top, middle, and bottom panels, respectively. The fluxes have been normalized to the continuum level close to the spectral lines. For each panel, the thick line with black dots and error bars is the observed profile for 96-BLG-3. The top panel shows the variation of the Hα line profile with temperature for three theoretical models with $T_{\rm eff}$ = 5800, 6000, and 6200 K. All three models have metallicity [M/H] = 0.3 and surface gravity log g = 4.0. As can be seen, the best-fit temperature is $T_{\rm eff} \approx$ 6100 K. The middle panel shows the variation of the Ca I + Fe I line region with metallicity for three theoretical models with [M/H] = 0.0, +0.3, +0.6 (*from top to bottom*). All the models have temperature $T_{\rm eff}$ = 6100 K and surface gravity log g = 4.0. Clearly the curve with low metallicity provides a poor fit, a value intermediate between [M/H] = +0.3 and +0.6 being appropriate. The bottom panel shows the variation of the Mg I triplet region with surface gravity for three theoretical models with log g = 3.5, 4.0, 4.5 (*from top to bottom*). All three models have temperature $T_{\rm eff}$ = 6100 K and metallicity [M/H] = +0.45 (*interpolated*). A surface gravity between log g = 4.0 and 4.5 provides the best fit at this metallicity. Note also the good fit to the other metal lines. (The discrepancy in the blue wing of the Mg I 5167.3 Å component is due to the neglect of C_2 opacity in the models.)

to determine the stellar radius. The resultant luminosity and bolometric magnitude are then used to derive the absolute visual magnitude using an assumed bolometric correction of −0.16, which is appropriate for a star of this temperature. In order to derive the distance we need also to compute the apparent magnitude corrected for extinction. We adopt an intrinsic $(V - R)_0$ = +0.47, the observed magnitude and color of V = 19.1 ± 0.1 and $(V - R)$ = 0.7 ± 0.05, leading to $E(V - R)$ = 0.23 and A_V = 0.91, for a standard extinction law in which R_V = 3.1. This is less than determinations of the mean extinction in Baade's window ($A_V \sim 1.5$; Paczyński et al. 1994), indicating that the extinction may vary significantly from the mean on small scales. The true distance modulus follows directly. The relevant quantities and the associated uncertainties are $M = 1.25^{-0.05}_{+0.20}\ M_\odot$, $R = 1.4^{-0.4}_{+0.6}\ R_\odot$, $M_{\rm bol}$ =

$3.8^{+0.7}_{-0.8}$, and distance $=6.9^{-1.7}_{+3.1}$ kpc. The given error estimates are dominated by the uncertainty in surface gravity (luminosity) and correspond to a reasonable change of ± 0.25 for $\log g$. We also note that the evolutionary tracks imply an age of $\leq 5 \times 10^9$ yr for 96-BLG-3.

4. DISCUSSION

It is necessary to consider how the derived stellar parameters might be compromised by the distortion of the normal center-to-limb variations caused by the lens. For this purpose we investigated the effect of lensing on a solar-type continuum and the Hα line. We chose the Hα line because it exhibits significant center-to-limb differences and modeled the effect of the lens on the intrinsic profile (using reasonable assumptions for unknown variables). We found that the expected change in the continuum in the three observations is $\lesssim 2\%$, while the expected change in the line profile is $\lesssim 1\%$ for the first spectrum, not enough to change the stellar parameters derived above. In fact, it should be emphasized that the very normality of the three spectrograms is compelling evidence that this is indeed a gravitational microlensing event.

The derived distance of 96-BLG-3 is clearly consistent with it lying in the bulge; nevertheless, it might also belong to the inner disk population. It is difficult to argue the case on kinematical grounds alone, particularly since little is known of the disk component at this distance. The large radial velocity would tend to favor the bulge population; indeed, 96-BLG-3 is consistent with the pattern found by Minniti (1996) of a correlation between mean galactocentric velocities and metallicity of bulge giants (the velocity dispersions are large nonetheless). However, it has been argued that the inner disk is kinematically hot (Lewis & Freeman 1989). In terms of metallicity, the recent spectroscopic analysis of bulge K giants in Baade's window by McWilliam & Rich (1994) implies that some stars have metallicities as high as [Fe/H] = +0.45 (see also Minniti et al. 1995). On the other hand, disk stars toward the Galactic center are also expected to be moderately metal rich if we consider the Galactic abundance gradient as inferred from H II regions (Simpson et al. 1995) and B-type supergiants (Smartt, Dufton, & Lennon 1996) toward the Galactic center. The resolution of this question may perhaps be achieved by consideration of the abundance pattern in 96-BLG-3 (note that we have assumed solar abundance ratios in the present analysis); field and bulge K-giants appear to exhibit differences in this respect (see McWilliam & Rich 1994). A future detailed spectrum synthesis of 96-BLG-3 (in progress) may shed further light on this problem. Furthermore, a combined study of the spectroscopic data and the photometric light curve should allow tighter constraints to be placed on the lensing parameters.

Mao & Paczyński (1991) estimated that about ~5%–10% of the microlensing events should exhibit binary features, which is roughly consistent with the observed fraction. With the upgrades of different experiments (such as the EROS and OGLE collaborations), the expected microlensing events will approach ≈ 100 events per year, which translates to about five caustic crossing events annually. With an 8–10 m class telescope, a S/N ratio of 100 can be readily achieved in less than 10 minutes of integration with 1 Å spectroscopic resolution. This means the stellar surface of the star can be studied with a resolution of $v_t(600\ \mathrm{s}) \approx 10^{10}$ cm $\approx 0.15\ R_\odot$, where we have taken the transverse velocity v_t to be 200 km s^{-1}. This provides a unique way to study the limb-darkening profiles of the continuum and the absorption lines, and perhaps even spots on the stellar surface and stellar chromospheres (see Loeb & Sasselov 1995 for a discussion of giants). Such microlensing events also provide important opportunities for studying the chemical compositions of the source stars in the Galactic bulge and, by implication, the nature and evolution of the bulge. These stars are normally beyond the reach of even 8–10 m class telescopes (at high resolution); however, the NTT 3.5 m telescope used here was briefly the largest in the world with an effective aperture size of 17.5 m!

This work would not have been possible without the prodigious effort of the MACHO collaboration and associate collaborator Sunhong Rhie in predicting the time of this caustic crossing. In particular, D. J. L. is indebted to Dave Bennett for a telephone call on the night of March 28 in the NTT control room informing him of the event! We also thank Peter Schneider for a careful reading of the manuscript and the ESO staff for their professional assistance with the observations. This project is partly supported by the "Sonderforschungsbereich 375-95 für Astro-Teilchenphysik" der Deutschen Forschungsgemeinschaft. We are indebted to an anonymous referee for providing us with improved unperturbed magnitudes for the 96-BLG-3 source star.

REFERENCES

Alard, C., et al. 1995, Messenger, 80, 31
Alard, C., Mao, S., & Guibert, J. 1995, A&A, 300, L17
Alcock, C., et al. 1993, Nature, 365, 621
———. 1996a, ApJ, 461, 84
———. 1996b, ApJ, submitted
———. 1996c, ApJ, in press
———. 1996d, ApJ, in press
———. 1996e, IAU Circ. 6361
Aubourg, E., et al. 1993, Nature, 365, 623
Benetti, S., Pasquini, L., & West, R. M. 1995, A&A, 294, L37
Bennett, D. P., et al. 1995, in AIP Conf. Proc. 336, Dark Matter, ed. S. S. Holt & C. L. Bennett (New York: AIP), 77
———. 1996, preprint (astro-ph 9606012)
Cayrel, R., Perrin, M.-N., Barbuy, B., & Buser, R. 1991, A&A, 247, 108
Dominik, M., & Hirshfeld, A. C. 1994, A&A, 289, L31
Fuhrmann, K., Axer, M., & Gehren, T. 1993, A&A, 271, 451
Fuhrmann, K., Pfeiffer, M., Frank, C., Reetz, J., & Gehren, T. 1996, in preparation
Lewis, J. R., & Freeman, K. C. 1989, AJ, 97, 139
Loeb, A., & Sasselov, D. 1995, ApJ, 449, L33
Mao, S., & Di Stefano, R. 1995, ApJ, 440, 22
Mao, S., & Paczyński, B. 1991, ApJ, 374, L37
McWilliam, A., & Rich, R. M. 1994, ApJS, 91, 749
Melnick, J., Dekker, H., & D'Odorico, S. 1994, ESO Operating Manual No. 15
Minniti, D. 1996, ApJ, 459, 579
Minniti, D., Olszewski, E. W., Liebert, J., White, S. D. M., Hill, J. M., & Irwin, M. J. 1995, MNRAS, 277, 1293
Paczyński, B. 1986, ApJ, 304, 1
———. 1996, ARA&A, in press
Paczyński, B., Stanek, K. Z., Udalski, A., Szymanski, M., Kaluzny, J., & Kubiak, M. 1994, AJ, 107, 2060
Pratt, M. 1996, talk presented at the Second Intl. Workshop on Gravitational Microlensing Surveys
Schaerer, D., Charbonnel, C., Meynet, G., Maeder, A., & Schaller, G. 1993, A&AS, 102, 339
Schaller, G., Schaerer, D., Meynet, G., & Maeder, A. 1992, A&AS, 96, 269
Simpson, J. P., Colgan, S. W. J., Rubin, R. H., Erickson, E. F., & Hass, M. R. 1995, ApJ, 444, 721
Smartt, S. J., Dufton, P. L., & Lennon, D. J. 1996, A&A, submitted
Udalski, A., et al. 1993, Acta Astron., 43, 289
———. 1994a, Acta Astron., 44, 165
Udalski, A., Szymanski, M., Kaluzny, J., Kubiak, M., Mateo, M., Krzeminski, W., & Paczyński, B. 1994b, Acta Astron., 44, 227
Udalski, A., Szymanski, M., Mao, S., Distefano, R. Kaluzny, J., Kubiak, M., Mateo, M., & Krzeminski, W. 1994c, ApJ, L103